Hsa_Circ_0054284 Functions as a Tumor Suppressor via The Mir-18a-3p/TIMP2 Pathway in Non−Small-Cell Lung Cancer

Zhexuan Xu
Zhengzhou University First Affiliated Hospital

Chunya Lu
Zhengzhou University First Affiliated Hospital

Guojun Zhang (✉ zgj@zzu.edu.cn)
Zhengzhou University First Affiliated Hospital   https://orcid.org/0000-0003-1756-0082

Abstract

Background: Non-small cell lung cancer (NSCLC) patients are basically at an advanced stage once diagnosed. In this study, our aimed to identify a new biomarker for early diagnosis of NSCLC.

Methods and materials: CircRNA array analysis was designed to study the expression patterns of circRNAs in three pairs of NSCLC tissues. The expression of hsa_circ_0054284 were detected in 30 paired NSCLC tissues and adjacent normal tissues by qRT-PCR assay. A549 and H520 cells were transfected with overexpression vector of hsa_circ_0054284 and negative control. CCK-8, transwell invasion and Cell apoptosis assay were using to explore the internal relationship among the hsa_circ_0054284, miR-18a-3p and TIMP2. TIMP2 expression level was detected by qRT-PCR assay and western blotting analysis.

Results: Hsa-circ-0054284 overexpression suppressed A549/H520 cell proliferation and invasion and promoted apoptosis via downregulation of miR-18a-3p and targeting TIMP2. This might be one of the possible mechanisms, which hsa-circ-0054284 plays in NSCLC.

Conclusion: The current study provides novel insights into the circRNA-related ceRNA network in NSCLC and the hsa-circ-0054284 biomarkers may be Early diagnosis in NSCLC patients.

Introduction

Lung cancer is one of the most common malignancies with the highest mortality rate in the world and poses a great threat to human health [1]. Histologically, there are two main types of lung cancer: small cell lung cancer and non-small cell lung cancer (NSCLC). NSCLC is the most common type of lung cancer, accounting for 80−85% of all lung cancer cases [2]. Surgical resection is the best treatment for lung cancer [3], however, the majority of patients were diagnosed with advanced stage, and the chemotherapy drugs had some effect on the treatment, but the overall 5-year survival rate did not really improve[4]. It has also been reported that the change of gene expression plays an important role in the occurrence and development of tumor. The study of oncogenes and tumor suppressor genes may provide important information for early diagnosis and treatment of cancer [5, 6]. Therefore, it is necessary to explore new unknown factors involved in the development of lung cancer so as to be able to early diagnosis and early treatment, which may improve patients' 5-year survival rate and quality of life.

Circular ribonucleic acid (CircRNA) is a circular endogenous RNA that is mainly formed by splicing the head and tail of an exon. It is stable in structure and has high tissue specificity. Further evidence suggests that circRNAs may act as a microRNA (miRNA) sponge to influence the expression of genes and proteins, thus affecting miRNA activity [7]. CircRNAs are more stable than other linear RNA regulators, which makes them basic research and may provide valuable ideas for clinical diagnosis and treatment in the future [8, 9]. Some circRNAs can be detected in peripheral blood and can be used as early diagnostic markers for many cancers, including lung cancer [10]. Then, exploring the potential role of circRNAs in cancer may help to verify therapeutic targets and develop new targeted therapeutic drugs [11, 12]. However, there are few reports on their role in NSCLC.

In our preliminary work, a circRNA microarray was performed by the Shanghai Biotechnology Corporation to analyze the differentially expressed circRNAs between three pairs of NSCLC tissues and adjacent normal lung tissues that we had collected. Among the dysregulated circRNAs, hsa_circ_0054284 had attracted our attention as bioinformatics analysis suggested that complimentary regions existed between hsa_circ_0054284 and miR-18a-3p, this means that has_circ_0054284 can play the role of ceRNA through adsorption of miR-18a-3p. It has been reported that miR-18a-3p is involved in the occurrence and development of lung cancer [13–16]. Bioinformatics and software analysis have also identified TIMP2 as a potential target gene for miR-18a-3p. TIMP2 has also been reported to be involved in cancer progression, including lung cancer [17–28].

In this study, we first verified the circular form of has_circ_0054284 by sequencing analysis. Then, the expression of has_circ_0054284 was confirmed in the tissue specimens of 30 patients with NSCLC. The effect of has_circ_0054284/miR-18a-3p/TIMP2 has not been studied. In order to explore the effect of this axis, we constructed has_circ_0054284 overexpression vector to explore the effects on proliferation, invasion and apoptosis of NSCLC cell lines A549 and H520. The possible mechanism was explored by bioinformatics technology and dual-luciferase reporter assays. Finally, we compared the effects of miR-18a-3p down-regulation and has_circ_0054284 overexpression to further determine the potential has_circ_0054284/ miR-18a-3p/TIMP2 axis in NSCLC.

Materials And Methods

Clinical-specimen collection

In total 30 tumor specimens and pair-matched adjacent normal tissues (5 cm from the edge of tumor) samples were collected from patients who were diagnosed with NSCLC and who had received a pulmonary segmentectomy from October 2017 to June 2018 in the First Affiliated Hospital of Zhengzhou University. The patients had not yet received any chemo or radiotherapy. Pathological diagnosis was based on biopsy after resection and confirmed by two experienced pathologists individually. After isolation, the tissues underwent rapid freezing in liquid nitrogen within 1 min and were stored in cryo freezer at −80°C before usage. As shown in Table 1, the clinical information of all the participants, including gender, age, smoking⊠differentiation, TNM stage, lymph node metastasis and pathologic types were recorded for further analysis. The research was approved by the Human Research Ethics Committee of Zhengzhou University. A written informed consent was obtained from each participant.

Cells and reagents

We purchased the NSCLC A549, luciferase-tagged A549, H520 and NHBE cell lines from the Cell Bank of Shanghai Institutes for Biological Sciences of the Chinese Academy of Sciences (Shanghai, China). Lentivirus expression vectors (pLO5-ciR) with hsa_circ_0054284 (Circ-Ex) or circ−normal-control (NC) fragments were obtained from Geneseed Biotech (Guangzhou, China). We purchased primary antibodies for Western blotting against the tissue inhibitor of metalloproteinases 2 (TIMP2; D18B7), glyceraldehyde

3-phosphate dehydrogenase (GAPDH; D16H11) and secondary antibody (7074P2) for Western blotting from Cell Signaling Technology (CST; Danvers, Massachusetts, US).

RNA library preparation and circRNA sequencing

We sent three pairs of NSCLC tissue samples (T1/N1, T2/N2 and T3/N3) to Sinotech Genomics Ltd (Shanghai, China) for RNA library preparation and circRNA sequencing. We used edgeR software (http://bioconductor.org/) to analyze differences in the expression of circRNAs between lung cancer tissues and normal tissues. For detailed steps, see the guidance provided by the company.

Cell culture and transfection

We cultured the cells with Dulbecco's Modified Eagle's Medium (DMEM; GIBCO [Thermo Fisher Scientific, Waltham, Massachusetts, USA]) containing 10% fetal bovine serum (FBS) and 1% penicillin–streptomycin (both GIBCO) in a humidified incubator (Thermo Fisher) under 5% CO_2 at 37° C. MiR-18a-3p mimics, miR-18a-3p inhibitors, miR-NC or si-TIMP2 (Shanghai GenePharma Co., Ltd., Shanghai, China) were transfected respectively or co-transfected according to different experimental groups. Cells of A549 and H520 were infected with lentivirus containing hsa_circ_0054284 (Circ-Ex group) or negative control fragment (Circ-NC group) and then selected by puromycin to obtain the stable hsa_circ_0054284/NC expressed cells (Hanbio, Shanghai, China). We harvested cells 24–72 hours after transfection for assays.

Cell Counting Kit-8 (CCK-8) assay

We seeded A549 and H520 cells into 96-well plates with 100 μl culture medium 24 hours after transfection. Each well was added with 10 μl CCK-8 solution (Dojindo Laboratories, Kumamoto, Japan) after culture for 0, 24, 48 or 72 hours per manufacturer's instructions. We measured OD_{450} values using a microplate reader (Bio-Rad Laboratories, Inc., Hercules, California, US) to detect cell viability. All experiments were conducted in triplicate.

Transwell invasion assay

A549 and H520 cells were cultured in 6-well plates at a cell density of $5×10^4$ cells/well in DMEM supplemented with 10% FBS. Cells were allowed to attach overnight at 37°C in a humidified atmosphere of 5% CO_2. After treating with circ-EX/NC, miR-Inhibitor/NC or transfection for 24 hours, cells of $5×10^4$ were seeded in the top compartment of 8 μm pores transwell culture inserts (Corning Life Sciences, Corning, NY, US) in the presence of serum free medium. Complete medium containing 20% FBS was added to the bottom compartment of the plate. After incubating, cells that had not migrated were removed from inside the transwell with a cotton swab; the outside cells were then fixed in cold methanol at room temperature for 30 min and stained with 0.05% crystal violet for 5 min. Aftering washing with PBS, the number of migrated cells present in the bottom compartment of each well was then determined using an inverted microscope. Three independent experiments were performed.

Cell apoptosis assay

Apoptotic cell numbers were detected by Annexin V-FITC/PI Apoptosis Detection Kit (Nanjing KeyGen Biotech Co. Ltd., Nanjing, China). Twenty-four hours after different treatment, cells were digested by trypsin without EDTA, and resuscitated at a concentration of 1×10^6 cells /mL in 1× binding buffer. Annexin V-FITC and PI were added into the binding buffer and well mixed. After 30 minutes incubation with room tempreture without light, the flow cytometry (BD Biosciences, San Diego, CA) was used to detect the signals of cells.

Xenograft mouse model

We packaged the recombinant lentiviruses Circ-Ex and Circ-NC and infected them into luciferase-tagged A549 cell lines. A stable transformed cell line was obtained by puromycin screening. Then, we subcutaneously injected cells (2×10^6) into the axillae of BALB/c nude mice bought from Beijing Vital River Laboratory Animal Technology Center (Beijing, China). Luciferase signals were obtained by a Xenogen IVIS Imaging System (Xenogen Corp., Alameda, California, USA). After 4 weeks, we sacrificed the mice, stripped and weighed the tumors, performed immunohistochemical (IHC) and also performed qRT-PCR. Our protocols were approved by the Animal Experimental Ethics Committee of Zhengzhou University.

Immunohistochemistry

The tissues obtained above were fixed in 4% formaldehyde and embedded in paraffin. Then 3-5 μm sections from all the tissues were cut using a freezing microtome (Thermo Scientific, Germany) and stained with hematoxylin/eosin (H&E) for pathological examination. For immunohistochemistry, tumor sections were incubated with primary antibody against Ki-67 (dilution 1:150; AF1738; Beyotime, Shanghai, China) were performed rinse, secondary antibody incubation (dilution 1:50; A0208; Beyotime), and dehydration following the manufacturer's instructions.

Dual-luciferase reporter assay

We obtained wild-type and mutant-type target gene fragments via PCR and overlap PCR amplification and then inserted them into the luciferase gene in pmirGLO promoter vector (Promega Life Sciences, Madison, Wisconsin, USA) to generate 4 pairs of recombinant plasmids: pmirGLO-Wt/Mt_circ_0054284; pmirGLO-Wt/Mt TIMP2 (pmirGLO-Wt1/Mt1; pmirGLO-Wt2/Mt2; pmirGLO-Wt3/Mt3). We plated 293T cells in 24-well plates and co-transfected them with the above recombinant plasmids and miRNAs (miR-18a-3p mimics, miR-Inhibitor or miR-NC) using Lipofectamine 2000. After 24 hours' transfection, we measured luciferase activities in each group per manufacturer's instructions.

Western blotting

After transfection for 48 h, western blotting was performed to detect protein expression level. The A549 and H520 cells were collected, washed with PBS, and lysed with RIPA and PMSF lysis buffer (Beyotime).

The total protein concentrations were detected by BCA protein assay kit (Beyotime). Fifty micrograms of protein from each group was exposed to SDS-PAGE and transferred onto polyvinylidene difluoride membranes. We used anti-GAPDH antibody as internal reference. After completing Western blotting per manufacturers' instructions, we assessed the protein bands using a Typhoon PhosphorImager system (GE Healthcare, Chicago, Illinois, USA).

Statistical analysis

In this study, we used SPSS software version 25.0 (SSPS Inc., Chicago, Illinois, USA) for all statistical analysis. Each experiment was repeated three times. Data are presented as mean ± standard deviation (SD). We used Student's t test and One-way ANOVA to assess differences between groups. $P < 0.05$ was considered statistically significant.

Results

1. CircRNA hsa_circ_0054284 expression was low in NSCLC cell lines and tissue samples

We performed a RNA library preparation and circRNA sequencing of tissue samples. The results showed that differentially expressed circRNAs with more than threefold change. In addition, hsa_circ_0054284 showed a significant decrease in the tumor group compared with the normal group (Fig. 1A). In order to prove that hsa_circ_0054284 exists in the form of a ring structure, we conducted a series of validation experiments on A549, H520 and NHBE cells and on NSCLC tissues. The results of sequence analysis showed that mature hsa_circ_0054284 was 375 bp long and consisted of exon 13 and part of exon 14 of the fork box metastasis-associated protein 3 (MTA3) gene. The above results were consistent with the Basic Local Alignment Search Tool (BLAST) outcomes and showed that the connection sequence does not exist. These indicated that the annular structure was formed by connecting the heads and tails of exon 13 and part of exon 14 (Fig. 1B). The above results confirmed the existence of hsa_circ_0054284.

In this study, qRT-PCR method was used to detect the expression of hsa_circ_0054284 in cancer and paracancerous tissues and A549 and H520 cell lines, and NHBE was used as control, which indicated that the expression of hsa_circ_0054284 in NSCLC was notably lower than that in paracancerous tissues, and that in A549 and H520 was markedly lower than that in NHBE cell lines.(P < 0.05; Fig. 1C). These results confirmed the low expression of hsa_circ_0054284 in NSCLC tissue samples and cell lines.

2. Effects of hsa_circ_0054284 overexpression on proliferation, invasion and apoptosis of NSCLC cells

To evaluate the effect of hsa_circ_0054284 on NSCLC, Lentivirus expression vectors expressing hsa_circ_0054284 (Circ-Ex) or Circ-NC were transfected them separately into A549 and H520 cells. Hsa_circ_0054284 expression increased after transfection, as shown by qRT-PCR, indicating successful transfection ($P < 0.05$; Fig. 2A). We designed 3 groups—Circ-Ex, Circ-NC and Blank—to explore the effects of hsa_circ_0054284. CCK-8 assay showed that Circ-Ex inhibited cell proliferation ($P < 0.05$; Fig. 2B◯C). In our Transwell experiments, Circ-Ex effectively inhibited the invasion ability of NSCLC cell lines ($P < 0.05$;

Fig. 2D). FCM assay results showed that hsa_circ_0054284 had a significant apoptosis-promoting effect in the Circ-Ex group comparison to Circ-NC group (P < 0.05; Fig. 2E).

3. Hsa_circ_0054284 overexpression inhibited the growth of A549 xenograft tumors *in vivo*

To our delight, the results of xenograft tumor growth experiments showed that hsa_circ_0054284 upregulation had an inhibitory effect on NSCLC in vivo.After inoculation with Circ-Ex, compared with the the Circ-NC group, total flux of luciferase signals of nude mice at 2, 3 and 4 weeks was observably lower, and signal strength was further reduced with time (P < 0.05; Fig. 3A). We observed same trend in tumor weights (P < 0.05; Fig. 3B). Next, we carried out the Ki-67 IHC experiment on the exfoliated tumor which showed that the positive rate of tumor cell proliferation markers in the Circ-Ex group was notably lower than in the Circ-NC group (P < 0.05; Fig. 3C). We also investigated whether hsa_circ_0054284 expression was increasing in A549 xenograft tumors by qRT-PCR. The expression of hsa_circ_0054284 in the Circ-Ex group was higher than that in the Circ-NC group (P < 0.05; Figure 3D).

4. Hsa_circ_0054284 could sponge miR-18a-3p and inhibit expression of miR-18a-3p

We found that hsa_circ_0054284 could absorb miR-18a-3p, and hsa_circ_0054284 had the binging sites with miR-18a-3p (Fig. 4A). MiR-18a-3p mimics and pmirGLO-Wt-circ_0054284 were cotransfected into 293T cells, the relative luciferase activity of this group was the lowest, but there was no obvious difference among the other three groups. (P < 0.05; Fig. 4B). We analyzed miR-18a-3p and hsa_circ_0054284 data in 30 NSCLC tissues and found that these two RNAs were negatively correlated in terms of expression (R^2 = 0.431, P < 0.05; Fig. 4C). Besides, qRT-PCR indicated that miR-18a-3p expression was downregulated in the Circ-Ex group transfected with upregulated hsa_circ_0054284 (P < 0.05; Fig. 4D). From the above, these results indicated that hsa_circ_0054284 overexpression may play a role by influencing miR-18a-3p.

5. Effects of miR-18a-3p inhibition on growth, invasion and apoptosis in A549 and H520 cells

We designed three groups—miR-Inhibitor, miR-NC and Blank—and then transfected them separately into A549 and H520 cells. qRT-PCR results indicating that the expression of miR-18a-3p decreased after transfection of the miR-Inhibitor group. (P < 0.05; Fig. 5A). Our cell proliferation assay manifested that miR-Inhibitor inhibited cell proliferation (P < 0.05; Fig. 5B, C). In Transwell experiments, miR-Inhibitor effectively restrained invasion ability in NSCLC cell lines (P < 0.05; Fig. 5D). FCM analysis showed that after transfection with miR-Inhibitor, the apoptosis rate of the 2 cell lines increased greatly compared with control group (P < 0.05; Fig. 5E).

6. TIMP2 was a target gene downstream of miR-18a-3p

The results of bioinformatics analysis using TargetScan and miRanda implied that TIMP2 mRNA shared three complementary matching regions with miR-18a-3p and might therefore be a potential target. (Fig. 6A). Furthermore, we verified this binding site through dual-luciferase reporter assays. Compared with the

control groups, we could know that fluorescence activity was markedly reduced in miR-18a-3p mimics and the wild-type pmirGLO co-transfection group but significantly increased in the miR-Inhibitor and wild-type pmirGLO co-transfection groups (P < 0.05; Fig. 6B1, B2), but, Figure 6B-3 showed that the third complementary site has no statistical significance. That is to say the first and second binding sites could effectively regulate the expression of TIMP2, while the third site had no obvious effect, suggesting that miR-18a-3p regulated TIMP2 expression by binding to the first and second sites. Then, Western blotting showed an apparent decrease in TIMP2 protein expression under miR-18a-3p mimic transfection (Fig. 6C), miR-18a-3p inhibitor can increase the expression of TIMP2. Taken together, our results showed that miR-18a-3p might have bound to the 3' untranslated region (UTR) of TIMP2 mRNA and downregulated TIMP2 protein expression level. In other words, TIMP2 was a target gene downstream of miR-18a-3p.

7. **Silenced TIMP2 (si-TIMP2) partly attenuated the effect of overexpression of hsa_circ_0054284 in A549 and H520 cells**

To further illustrate the existence of the hsa_circ_0054284/miR-18a-3p/TIMP2 pathway, we synthesized a silenced RNA (si-RNA) of TIMP2 and performed a restoration experiment using a Transwell assay. We designed eight groups: Blank, Circ-NC only, miR-NC only, Circ-Ex transfection only, miR-Inhibitor transfection only, si-TIMP2 transfection only, Circ-Ex−si-TIMP co-transfection and miR-Inhibitor−si-TIMP co-transfection. When compared with Circ-Ex/miR-Inhibitor only cells, the combination group (Circ-Ex−si-TIMP2/miR-Inhibitor−si-TIMP) showed fewer inhibitory effects of invasion in 2 cell lines (P < 0.05; Fig. 7A), which indicated that si-TIMP2 partially restored the effects of hsa_circ_0054284 overexpression and miR-18a-3p inhibitor. Figure 7B showed a schematic diagram of the mechanism of circRNA action. Summary, we could conclude that (1) hsa_circ_0054284 overexpression downregulated the expression of miR-18a-3p, (2) miR-18a-3p targeted TIMP2, (3) hsa_circ_0054284 overexpression inhibited cell growth and invasion and promoted apoptosis in NSCLC cells, and (4) these tumor-inhibitory effects might have been exerted through the hsa_circ_0054284/miR-18a-3p/TIMP2 pathway.

Discussion

In recent years, research on ncRNA has become a hot topic. Various evidences indicate that ncRNA may play a role as a regulatory network. CircRNA is also a new type of ncRNA, which may play a key role in ncRNA network because of its stable ring structure and resistance to RNA enzyme [29, 30]. CircRNAs have been reported to be involved in a variety of physiological and pathological processes, including aging, various diseases and malignancies [31-35]. CircRNAs have been reported to be associated with the development and progression of lung cancer [36, 37]. In this study, we screened out a new circRNA (hsa_circ_0054284) by technical means, and carried out a series of studies to explore the role and potential mechanism of hsa_circ_0054284 in lung cancer.

First, we confirmed the existence of circular hsa_circ_0054284 by sequencing analysis, and detected the expression of hsa_circ_0054284 in cell lines and 30 clinical samples. As shown by qRT-PCR, the expression of hsa_circ_0054284 in cancer tissues was lower than that in paracancerous tissues.

Compared with NHBE cell line, hsa_circ_0054284 was expressed lower in A549 and H520 cells. Low expression of hsa_circ_0054284 was also associated with tumor differentiation, TNM stage, and lymph node metastasis. Therefore, we predict that hsa_circ_0054284 may be related to the prognosis of NSCLC. Then, we explore the relevant regulatory networks around hsa_circ_0054284 and find that miR-18a-3p is a potential target. It has been reported that miR-18a-3p is involved in the occurrence and development of tumor [38]. MiR-18a-3p acts as a tumor suppressor gene in some cancers, such as esophageal cancer and ovarian cancer [39, 40]. But in lung cancer, miR-18a-3p is an oncogene [41]. In our study, we found that hsa_circ_0054284 can negatively regulate miR-18a-3p. Fig. 4C, D results show that overexpression of hsa_circ_0054284 leads to a decrease in the expression of miR-18a-3p. TIMP2 was identified as a potential target for miR-18a-3p. Tissue inhibitor of metalloproteinases-2 (TIMP2) is a broad spectrum inhibitor of the matrix metalloproteinases (MMPs) [42]. It has been reported that TIMP2 is associated with cancer progression, such as oropharyngeal carcinoma and breast cancer [43, 44].TIMP2 plays a role in inhibiting cancer progression in lung cancer [45-47].

Finally, a series of verification experiments show that the previous conjecture is reasonable. In this study, we screened a low expression circRNA(hsa_circ_0054284), according to the results of the chip, and then verified its expression trend in tissue samples to verify whether the expression trend was consistent with the results of the chip, and then verified in a variety of cell lines. Both show that hsa_circ_0054284 is low expression, so we constructed a circRNA overexpression vector(circ-EX) to carry out the next series of exploratory experiments. As shown in Fig.2, overexpression of hsa_circ_0054284 can inhibit proliferation and invasion but promote apoptosis. MiR-18a-3p downregulation also has the above effect, see Fig.5. As shown in Fig.4A, B, C, D, it shows that hsa_circ_0054284 can adsorb miR-18a-3p to exert the function of ceRNA, thus negatively regulating miR-18a-3p. In figure 6, the dual-luciferase reporter and western blotting experiments confirmed that TIMP2 is the target gene of miR-18a-3p, that is to say, miR-18a-3p can negatively regulate TIMP2. Silencing TIMP2 can increase invasion. It has been reported that TIMP2 is related to proliferation and apoptosis. However, silencing TIMP2 can partially restore the overexpression of hsa_circ_0054284 and the inhibitory effect of miR-18a-3p inhibitor on invasion, see Fig.7. In conclusion, the hsa_circ_0054284 / miR-18a-3p / TIMP2 axis exists.

To sum up, this study suggests that hsa_circ_0054284 may inhibit cell growth and invasion and promote apoptosis by down-regulating miR-18a-3p and targeting TIMP2. Hsa_circ_0054284/ miR-18a-3p/ TIMP2 axis exists. Hsa_circ_0054284 can be used as a potential prognostic biomarker and therapeutic target for NSCLC. However, other approaches are likely to be involved, and future studies will explore alternative ways of action.

Conclusion

Hsa-circ-0054284 overexpression suppressed A549/H520 cell proliferation and invasion and promoted apoptosis via downregulation of miR-18a-3p and targeting TIMP2. This might be one of the possible mechanisms, which hsa-circ-0054284 plays in NSCLC.

Declarations

Ethics approval and consent to participate

Not applicable.

Consent for publication

Not applicable.

Competing interests

No conflict of interest.

Acknowledgments

We would like to thank department of respiratory and critical care medicine, The first affiliated hospital of Zhengzhou University for academic support. We thank LetPub (www.letpub.com) for its linguistic assistance during the preparation of this manuscript.

Authors' contributions

Guojun Zhang, Zhexuan Xu designed the study. Zhexuan Xu finished a majority of experiments and analyzed the data. Chunya Lu collected NSCLC tissue samples. Zhexuan Xu and Chunya Lu wrote the manuscript. All authors read and approved the submitted version.

Funding

Availability of data and materials

The data used to support the findings of this study are included within the article.

References

1. Bray F, Ferlay J, Soerjomataram I. **et al**. Global cancer statistics 2018: GLOBOCAN estimates of incidence and mortality worldwide for 36 cancers in 185 countries. CA Cancer J Clin. 2018;68:394–424.

2. Ettinger DS, Akerley W, Borghaei H. **et al**. Non–small cell lung cancer, version 2.2013. J Natl Compr Canc Netw. 2013;11:645–53.

3. Robles AI, Harris CC. Integration of multiple "OMIC" biomarkers: A precision medicine strategy for lung cancer. Lung Cancer. 2017;107:50–8.

4. Giovannetti E, Toffalorio F. **et al**. Pharmacogenetics of conventional chemotherapy in non-small-cell lung cancer: a changing landscape? Pharmacogenomics. 2012;13(9):1073–86., **De** Pas T.

5. Mazzone PJ, Sears CR, Arenberg DA. **et al**. Evaluating Molecular Biomarkers for the Early Detection of Lung Cancer: When Is a Biomarker Ready for Clinical Use? An Official American Thoracic Society Policy Statement. Am J Respir Crit Care Med. 2017;196(7):e15–29.

6. Hundal J, Carreno BM, Petti AA. **et al**. pVAC-Seq: A genome-guided in silico approach to identifying tumor neoantigens. Genome medicine. 2016;8(1):11.

7. Hansen TB, Jensen TI, Clausen BH. **et al**. Natural RNA circles function as efficient microRNA sponges. Nature. 2013;495:384–8.

8. Memczak S, Jens M, Elefsinioti A. **et al**. Circular RNAs are a large class of animal RNAs with regulatory potency. Nature. 2013;495(7441):333.

9. Yao T, Chen Q, Fu L. **et al**. Circular RNAs: biogenesis, properties, roles, and their relationships with liver diseases. Hepatol Res. 2017;47(6):497–504.

10. Mu Y, Xie F, Huang YF. **et al**. Circular RNA expression profile in peripheral whole blood of lung adenocarcinoma by high: Throughput sequencing. Medicine. 2019;98(42):e17601.

11. Cheng Y, Sun H, Wang H. **et al**. Star Circular RNAs In Human Cancer: Progress and Perspectives. OncoTargets therapy. 2019;12:8249.

12. Liu YT, Han XH, Xing PY. **et al**. Circular RNA profiling identified as a biomarker for predicting the efficacy of Gefitinib therapy for non-small cell lung cancer. Journal of thoracic disease. 2019;11(5):1779.

13. Xiao H, Liu Y, Liang P. **et al**. TP53TG1 enhances cisplatin sensitivity of non-small cell lung cancer cells through regulating miR-18a/PTEN axis. Cell bioscience. 2018;8(1):23.

14. Xu X, Zhu S, Tao Z. **et al**. High circulating miR-18a, miR-20a, and miR-92a expression correlates with poor prognosis in patients with non-small cell lung cancer. Cancer medicine. 2018;7(1):21–31.

15. Shen Z, Wu X, Wang Z. **et al**. Effect of miR-18a overexpression on the radiosensitivity of non-small cell lung cancer. Int J Clin Exp Pathol. 2015;8(1):643.

16. Tsang WP. **Kwok T T.** The miR-18a* microRNA functions as a potential tumor suppressor by targeting on K-Ras. Carcinogenesis. 2009;30(6):953–9.

17. Zeng XY, Jiang XY, Yong JH. **et al**. lncRNA ABHD11-AS1, regulated by the EGFR pathway, contributes to the ovarian cancer tumorigenesis by epigenetically suppressing TIMP2. *Cancer Medicine*. 2019.

18. Zhang X, Gong J, Lu J. **et al**. Long noncoding RNA LINC00337 accelerates the non-small-cell lung cancer progression through inhibiting TIMP2 by recruiting DNMT1. American Journal of Translational Research. 2019;11(9):6075.

19. Zhang G, Wang Q, Zhang X. **et al**. LncRNA FENDRR suppresses the progression of NSCLC via regulating miR-761/TIMP2 axis. Biomed Pharmacother. 2019;118:109309.

20. Yuan C. miR616 promotes breast cancer migration and invasion by targeting TIMP2 and regulating MMP signaling. Oncology letters. 2019;18(3):2348–55.

21. Li Q, Xing W, Gong X. et al. Long Non-Coding RNA Urothelial Carcinoma Associated 1 Promotes Proliferation, Migration and Invasion of Osteosarcoma Cells by Regulating microRNA-182. Cell Physiol Biochem. 2018;51(3):1149–63.

22. Chen A, Liu S, Lu X. et al. Inhibition of microRNA939 suppresses the development of human nonsmall cell lung cancer via the upregulation of tissue inhibitor of metalloproteinases 2. Mol Med Rep. 2018;18(6):4831–8.

23. Yang JZ, Bian L, Hou JG. et al. MiR-550a-3p promotes non-small cell lung cancer cell proliferation and metastasis through down-regulating TIMP2. Eur Rev Med Pharmacol Sci. 2018;22(13):4156–65.

24. Yosef G, Arkadash V, Papo N. Targeting the MMP-14/MMP-2/integrin αvβ3 axis with multispecific N-TIMP2–based antagonists for cancer therapy. J Biol Chem. 2018;293(34):13310–26.

25. Yang X, Zhang W, Cheng SQ. et al. High expression of lncRNA GACAT3 inhibits invasion and metastasis of non-small cell lung cancer to enhance the effect of radiotherapy. Eur Rev Med Pharmacol Sci. 2018;22:1315–22.

26. Guan H, Li W, Li Y. et al. MicroRNA-93 promotes proliferation and metastasis of gastric cancer via targeting TIMP2. PloS one. 2017;12(12):e0189490.

27. Sandoval-Bórquez A, Polakovicova I, Carrasco-Véliz N. et al. MicroRNA-335-5p is a potential suppressor of metastasis and invasion in gastric cancer. Clinical epigenetics. 2017;9(1):114.

28. Yan A, Yang C, Chen Z. et al. MiR-761 promotes progression and metastasis of non-small cell lung cancer by targeting ING4 and TIMP2. Cell Physiol Biochem. 2015;37(1):55–66.

29. Liu J, Liu T, Wang X. et al. Circles reshaping the RNA world: from waste to treasure. Mol Cancer. 2017;16(1):58.

30. Chen B, Huang S, Circular RNA. An emerging non-coding RNA as a regulator and biomarker in cancer. Cancer letters. 2018;418:41–50.

31. Zang J, Lu D, Xu A. The interaction of circRNAs and RNA binding proteins: An important part of circRNA maintenance and function. Journal of neuroscience research, 2018.

32. Knupp D, Miura P. CircRNA accumulation: A new hallmark of aging? Mech Ageing Dev. 2018;173:71–9.

33. Shafabakhsh R, Mirhosseini N, Chaichian S. et al. Could circRNA be a new biomarker for pre-eclampsia? Molecular reproduction and development, 2019.

34. Kumar L, Haque R, Baghel T. et al. Circular RNAs: the emerging class of non-coding RNAs and their potential role in human neurodegenerative diseases. Mol Neurobiol. 2017;54(9):7224–34.

35. Meng S, Zhou H, Feng Z. et al. CircRNA: functions and properties of a novel potential biomarker for cancer. Mol Cancer. 2017;16(1):94.

36. Braicu C, Zimta AA, Harangus A. et al. The function of non-coding RNAs in lung cancer tumorigenesis. Cancers. 2019;11(5):605.

37. De Fraipont F, Gazzeri S, Cho W. et al. Circular RNAs and RNA splice variants as biomarkers for prognosis and therapeutic response in the liquid biopsies of lung cancer patients. Frontiers in

genetics. 2019;10:390.

38. Guil S, Cáceres JF. The multifunctional RNA-binding protein hnRNP A1 is required for processing of miR-18a. Nat Struct Mol Biol. 2007;14(7):591.

39. Hummel R, Sie C, Watson DI. et al. MicroRNA signatures in chemotherapy resistant esophageal cancer cell lines. World journal of gastroenterology: WJG. 2014;20(40):14904.

40. Rodriguez-Aguayo C, del C Monroig P, Redis RS, et al. Regulation of hnRNPA1 by microRNAs controls the miR-18a–K-RAS axis in chemotherapy-resistant ovarian cancer. Cell discovery, 2017, 3: 17029.

41. Xiao H, Liu Y, Liang P. et al. TP53TG1 enhances cisplatin sensitivity of non-small cell lung cancer cells through regulating miR-18a/PTEN axis. Cell bioscience. 2018;8(1):23.

42. Bahudhanapati H, Zhang Y, Sidhu SS. et al. Phage display of tissue inhibitor of metalloproteinases-2 (TIMP-2) identification of selective inhibitors of collagenase-1 (metalloproteinase 1 (MMP-1)). J Biol Chem. 2011;286(36):31761–70.

43. Burduk PK, Bodnar M, Sawicki P. et al. Expression of metalloproteinases 2 and 9 and tissue inhibitors 1 and 2 as predictors of lymph node metastases in oropharyngeal squamous cell carcinoma. Head Neck. 2015;37(3):418–22.

44. Casar JM, D S, González-Reyes LO, González. et al. Expression of metalloproteases and their inhibitors in different histological types of breast cancer. J Cancer Res Clin Oncol. 2010;136(6):811–9.

45. Yin Z, Xu M, Li P. miRNA-221 acts as an oncogenic role by directly targeting TIMP2 in non-small-cell lung carcinoma. Gene. 2017;620:46–53.

46. Xu J, Du Y, Liu XJ. et al. Recombinant EGFR/MMP-2 bi-targeted fusion protein markedly binding to non-small-cell lung carcinoma and exerting potent therapeutic efficacy. Pharmacological research. 2017;126:66–76.

47. Yan A, Yang C, Chen Z. et al. MiR-761 promotes progression and metastasis of non-small cell lung cancer by targeting ING4 and TIMP2. Cell Physiol Biochem. 2015;37(1):55–66.

Tables

Table 1 is not available with this version.

Figures
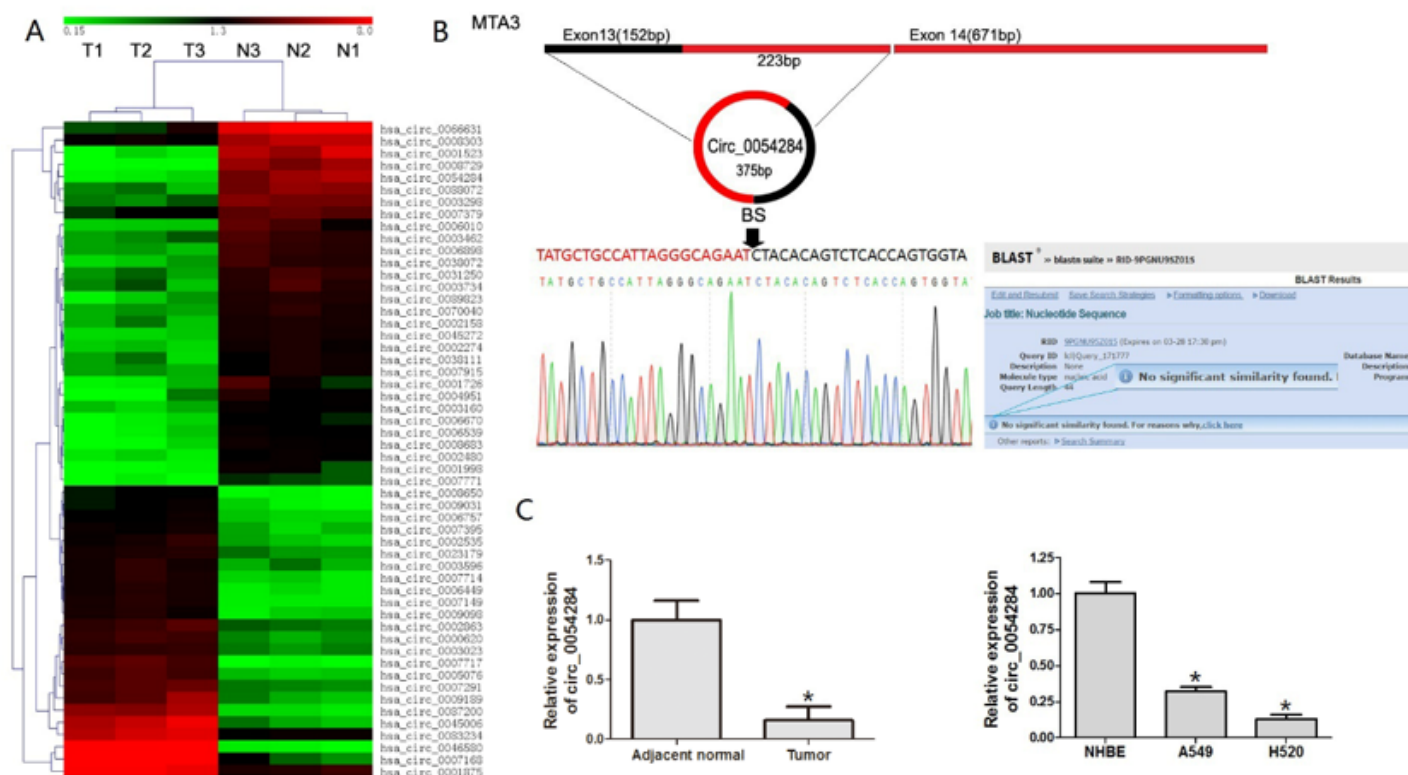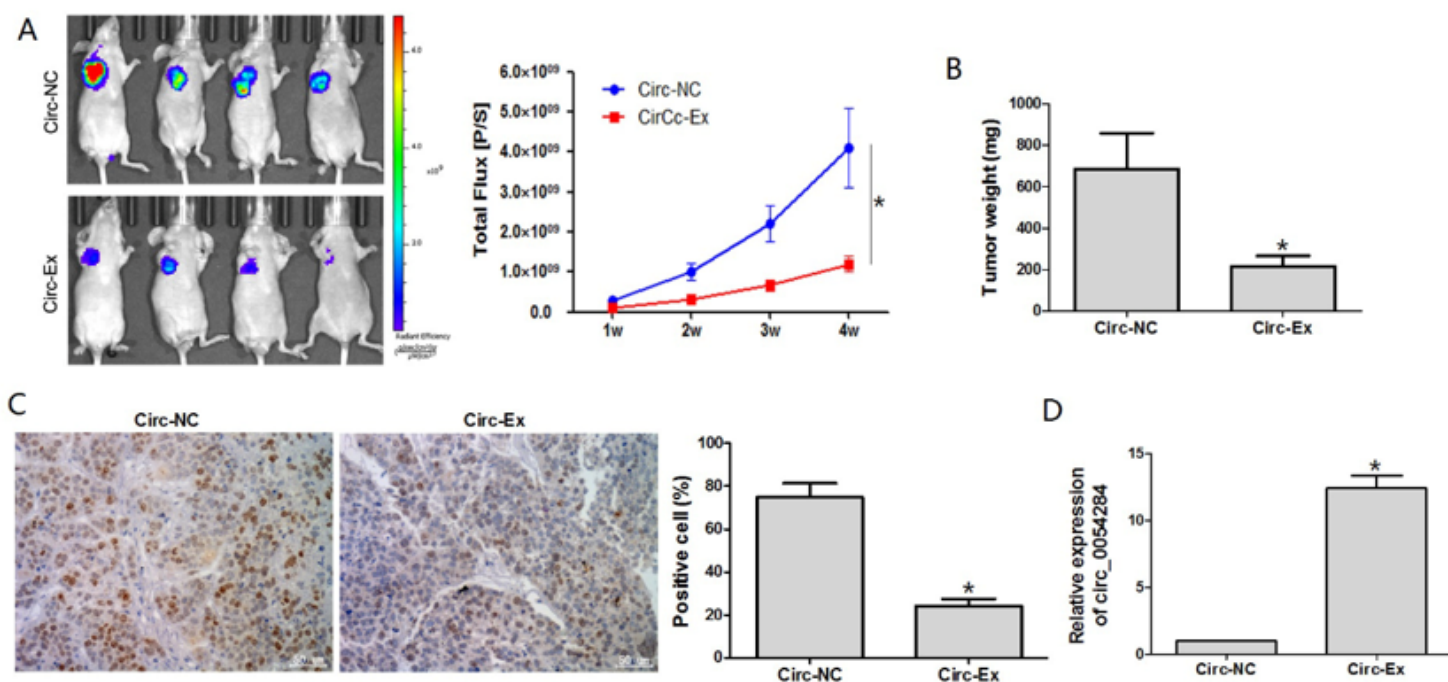
Figure 1

Hsa_circ_0054284 is present and down-regulated in NSCLC tissues and cells. (A) Heat map of circRNA array in NSCLC tumor samples. (B) Source of hsa_circ_0054284 and sequence analysis of backsplicing site site. (C) qRT-PCR showed that expression of hsa_circ_0054284 in cancer, paracancerous tissues and 2 cell lines. *P < 0.05 compared with the control group.
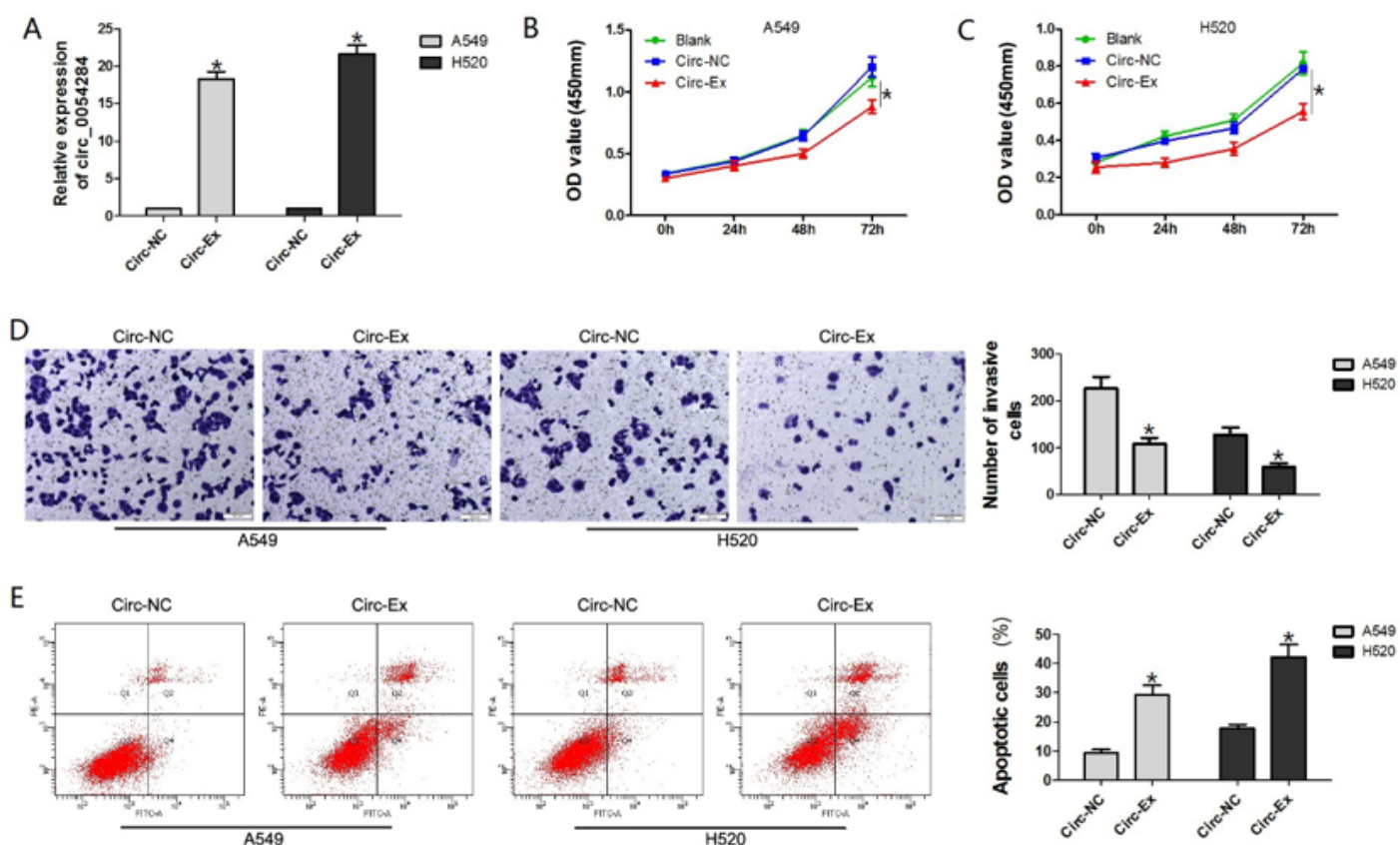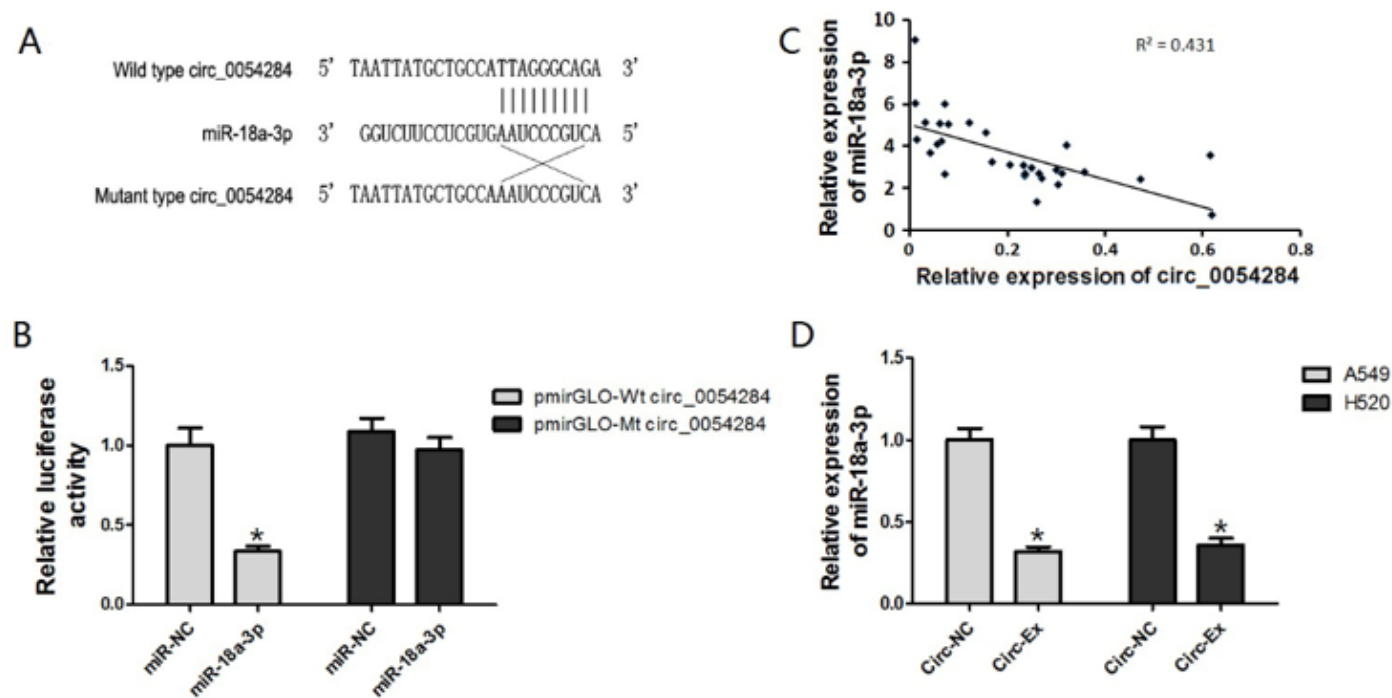
Figure 2

Overexpression of hsa_circ_0054284 inhibited cell proliferation and invasion and promoted cell apoptosis. (A) We detected the relative expression of hsa_circ_0054284 in A549 and H520 cells using qRT-PCR. (B, C) We conducted CCK-8 assays on different cell lines; the optical-density (OD) value showed that Circ-Ex could inhibit cell proliferation. (D) The effect of Circ-Ex could inhibit cell invasion using Transwell assays. (E) We measured apoptosis of A549 and H520 cells by staining them with Annexin V–FITC/PI, followed by FCM analysis showed that Circ-Ex could promote apoptosis. $*P < 0.05$. All data are representative of at least three independent experiments and presented as means ± SD.
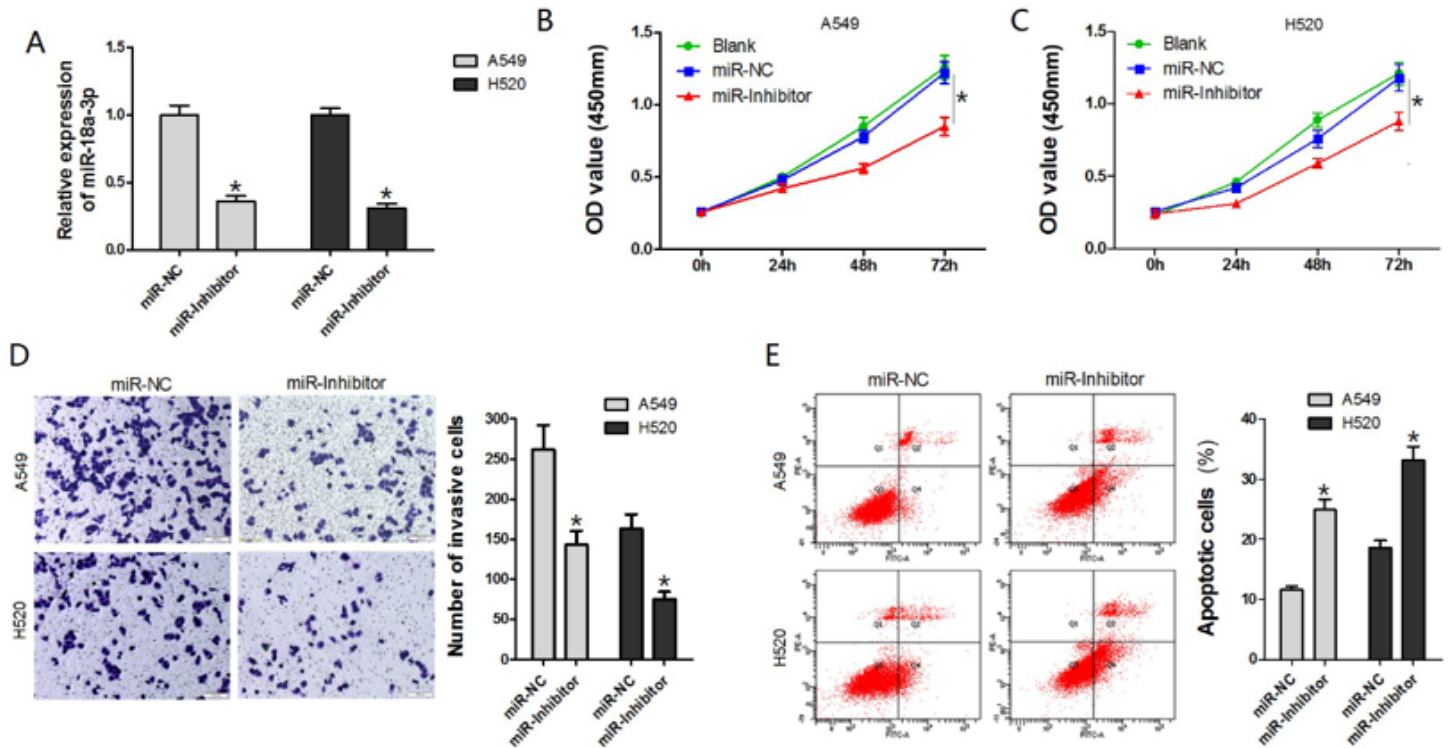
Figure 3

Effects of hsa_circ_0054284 overexpression in A549 xenograft mice. (A, B) Mice with xenograft tumors were divided into 2 groups, Circ-Ex and Circ-NC. We observed the weekly total flux of luciferase signals of each group and recorded tumor weight at week 4. (C) IHC staining using primary antibody against Ki-67. (D) hsa_circ_0054284 expression in A549 mouse xenograft. *$P < 0.05$.
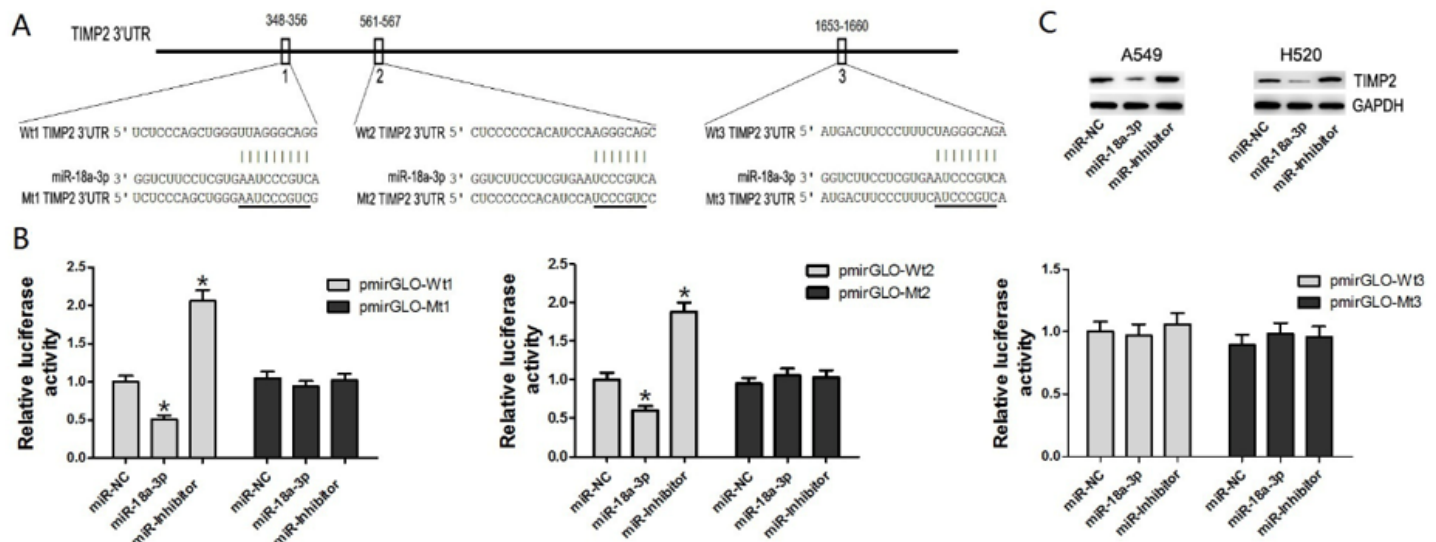

Figure 4

miR-18a-3p was a target o f hsa_circ_0054284. (A) Complementary binding site between the two. (B) A dual-luciferase reporter assay identified miR-18a-3p as a direct target miRNA of hsa_circ_0054284. (C) Expression of miR-18a-3p was negatively correlated with that of hsa_circ_0054284 ($R^2 = 0.431$, $P < 0.05$). (D) We applied qRT-PCR to investigate miR-18a-3p expression in cells treated with Circ-Ex, which showed that miR-18a-3p expression was downregulated in the Circ-Ex group. *P < 0.05.
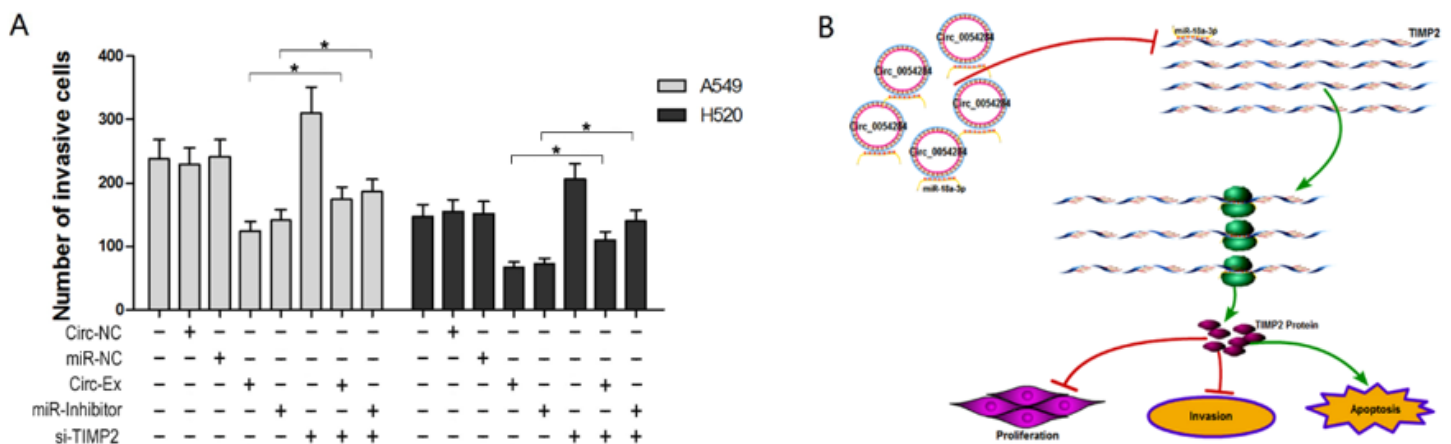

Figure 5

miR-18a-3p inhibition could inhibit proliferation and invasion and promote apoptosis in A549 and H520 cells. (A) Using qRT-PCR, we detected the expression of miR-18a-3p after treatment with miR-Inhibitor. (B, C) Proliferation of A549 and H520 cells in the miR-Inhibitor group was significantly lower than in the miR-NC and Blank groups (P < 0.05). (D) We detected cell invasion ability using a Transwell assay 24 hours after transfection with miR-Inhibitor. (E) Statistical increases can be seen in the number of apoptotic cells in miR-Inhibitor–transfected A549 and H520 cells compared with cells in the miR-NC group (P < 0.05). These results suggested that the effect of miR-Inhibitor on A549 and H520 cell lines was similar to that of Circ-Ex. *P < 0.05 compared with the control group.

Figure 6

TIMP2 was directly targeted by miR-18a-3p. (A) There were three seed regions for miR-18a-3p in the 3'-UTR of TIMP2 mRNA. (B) The dual-luciferase reporter assay confirmed TIMP2 acted as the target of miR-18a-3p. (C) Western blotting showed that protein levels of TIMP2 was decreased under miR-18a-3p mimic transfection. *$P < 0.05$.

Figure 7

Silencing of TIMP2 attenuated the effects of invasion with Circ-Ex and miR-Inhibitor on A549 and H520 cells. (A) It indicated that si-TIMP2 partially restored the effects of hsa_circ_0054284 overexpression and miR-18a-3p inhibitor. (B) a schematic diagram of the mechanism of circRNA action.

Supplementary Files

This is a list of supplementary files associated with this preprint. Click to download.

- originaldata.xlsx